Luminous Infra-Red Galaxy Inventory (LIRGI)

Coordinators: J.E.Conway (John.Conway@chalmers.se) & M.A. Perez-Torres (torres@iaa.es)

Address: J. E. Conway, Onsala Space Observatory, Onsala, SE-43992, Sweden, Phone +46-31-772-5503

Miguel A. Perez-Torres, IAA – CSIC, Granada, E-18008, Spain, Phone +34-958-230-644

ABSTRACT We propose legacy survey observations of 42 of the most luminous northern luminous infra-red galaxies selected from the IRAS revised Bright Galaxy Sample (Sanders et al. 2003). This survey will provide a high spatial resolution radio complement to legacy observations made with the NASA Great Observatories (GOALS program). Additionally it will itself provide legacy data to be combined with upcoming radio/millimetre/submm instruments. Our sample selects sources with L= log(Lir/Lsol) >11.4, which have sizes well matched to eMERLIN spatial resolution. The sample spans the range of FIR luminosities from the upper end of the Luminous Infra-Red Galaxies (LIRGs) to Ultra-Luminous Infra-Red Galaxies (ULIRGs), most of which are merging or post merger systems. Our local (<200 Mpc) targets have properties of area star formation densities, gas and radiation densities similar to star-forming galaxies at high redshift. A major goal of future radio/millimetre instruments is to use these high redshift objects to trace the star-formation (and galaxy assembly) history of the universe. Achieving this goal reliably requires understanding the physics of similar local objects. Crucially it is important to understand how accurately radio continuum flux densities can be converted to Star Formation Rates (SFR). If for instance in the warm dense gas environments of (U)LIRGs) the stellar Initial Mass Functions is top-heavy, the calibration of SFR from star-formation tracers can be affected. Definite evidence for non-standard IMFs in extreme environments would also be an important input into understanding star-formation mechanisms in general.

Specific project goals are: (1) To map the size and morphology of diffuse radio emission in each source at two wavelengths (6 cm and 18 cm). These observations will give the best estimate at any waveband of the physical size of the starburst, trace the free-free absorption, look for the predicted upper limits on radio brightness, etc. (2) Use three epoch 6 cm observations on a 25 source subsample to detect powerful core-collapse radio supernovae (RSNe) in order to constrain the high mass star-formation rate and hence the IMF. (3) Make polarisation and rotation measure observations to constrain the magnetic field properties, in order to check whether B fields are weak and in equipartition with relativistic particles, or are strong and in equipartition with the thermal gas. (4) Systematically study the gas dynamics and physical conditions at high angular resolution by observing absorption/megamaser spectral line emission (e.g. HI and four OH lines at L-band and OH and H_2CO at C-band). (5) Check for lobe, jet and core structures consistent from embedded AGNs. (6) Establish a phenomenological sequence and time scale for the evolution of a nuclear starburst using the combined FIR, continuum, and spectral line information provided by this Legacy survey.

Our proposed observations will consist of an initial epoch (semester 1) of quasi-simultaneous observations at L- and C-band of all 42 objects with 5 hrs per source per frequency (total 410 hrs). This will be followed by two additional epochs spaced one year apart (in semesters 3 and 5) of 25 sources at C-band to search for RSNe (total 250 hrs). Hence the total time request is 660 hrs. Our proposal will leave an important legacy to the community: a uniformly observed sample of (U)LIRGs in the nearby universe, done in a timely way that will serve as a reference for future studies to be carried out with forthcoming instruments (ALMA, EVLA, LOFAR, Herschel etc).

Complete list of team members

Susanne Aalto (Onsala Space Observatory, Chalmers, Sweden) [saalto@chalmers.se]
Antxon Alberdi (IAA, Granada, Spain) [antxon@iaaa.es]
Phil Appleton (NASA Herschel Science Center, Caltech USA) [apple@ipac.caltech.edu]
Willem Baan (ASTRON, The Netherlands) [baan@astron.nl]
Fabien Batejat (Onsala Space Observatory, Chalmers. Sweden) [Fabien.Batejat@chalmers.se]
Rob Beswick (JBCA, Manchester) [Robert.Beswick@manchester.ac.uk]
Luis Colina (DAMIR, Madrid, Spain) [colina@damir.iem.csic.es]
John Conway (Onsala Space Observatory, Chalmers, Sweden) [john.conway@chalmers.se]
Phil Diamond (JBCA, Manchester) [Phil.Diamond@manchester.ac.uk]
Denise Gabuzda (University College Cork, Ireland) [gabuzda@physics.ucc.ie]
Simon Garrington (JBCA, Manchester) [stg@jb.man.ac.uk]
Rossa Hurley (Onsala Space Observatory, Chalmers Sweden) [rossa@chalmers.se]
Hans-Rainer Klockner (Oxford) [hrk@astro.ox.ac.uk]
Carole Mundell (Liverpool, John Moores Univ) [cgm@astro.livjm.ac.uk]
Ray Norris (CSIRO, Australia) [ray.norris@csiro.au]
Miguel Perez-Torres (IAA, Granada, Spain) [torres@iaa.es]
Rodrigo Parra (Catolica Univ, Santiago, Chile) [rparra@astro.puc.cl]
Ylva Pihlström (Univ of New Mexico, USA) [ylva@unm.edu]
Cristina Romero-Canizales (IAA, Spain) [cromero@iaa.es]
Jose-María Torrelles (CSIC-IEEC, Barcelona, Spain) [torrelles@ieec.fcr.es]

A) Scientific Justification

1. Introduction

A major science goal for the SKA and its pathfinders is to use radio continuum and spectral line observations of high red-shift galaxies to study the galaxy formation and evolution process across cosmic time. Such observations can be used to infer the star-formation history of the universe, to establish the redshift of the first proto-galaxies, and to follow the process of the assembly of these small pieces to form the massive galaxies that we see today. However, these goals can be achieved only if we can properly interpret the diagnostic tools that are provided by the radio continuum and spectral line observations. As an example, to reliably trace star-formation via radio continuum we require that: (1) the empirically observed radio to infra-red correlations is a robust tool that remains valid (or whose variations can be calibrated) at all red-shifts and for a wide range of galaxy types (see Appleton et al. 2003; Beswick et al. 2008), and (2) that we can reliably convert from IR luminosities to star-formation rates measured in solar masses per year, which requires a stellar IMF that is stable or whose variations are understood. Given the importance of the IR-radio correlation tool, it is vital that we try to understand the detailed source physics underlying this correlation. Likewise observations are vitally needed to check the universality of the stellar IMF in dense environments and to interpret high z spectral line ratios.

Our proposed eMERLIN observations of nearby powerful star-forming galaxies can make valuable contributions to the above issues. They can for example be used to test the details of the standard mixed synchrotron-thermal plasma model for the starburst continuum emission. They can also be used to constrain internal magnetic field strengths and test whether calorimeter models can best explain the IR to radio correlation. Our observations can constrain the stellar IMF via radio SNe observations. Finally we can observe HI, OH and H_2CO spectral lines to constrain dynamics and chemistry. Spitzer observations show that at increasing redshift an ever-larger fraction of the star-formation occurs in luminous systems (Perez-Gonzales et al. 2005). It is therefore natural for us to observe the closest luminous sources with the most extreme physical conditions. Although these may not be exact templates of high red-shift systems (Norris et al. 2008), the closest Luminous and Ultra-luminous Infra-Red Galaxies or (U)LIRGs provide the best local examples that we have of the physical processes that are occurring at high redshift and are therefore worthy of detailed study.

2. Sample selection and properties

2.1 Source sample – We propose to observe the nearest powerful (U)LIRGs in the universe having luminosity log(Lir/Lsol) >11.4. This luminosity cut-off primarily selects compact sources (d<500pc), which have the most extreme physical conditions, and therefore provide the best tests of the universality of star-formation properties. At our chosen minimum luminosity, the contribution to the luminosity from the normal optically selected galaxy population falls off rapidly and a new high luminosity tail population starts to dominate (Sanders et al 2003). Finally at this luminosity, we observe the transition from mainly isolated galaxies to mostly interacting and merging systems (Sanders & Ishida 2004). Our choice of luminosity cut-off therefore allows us to select the local analogues of the luminous merger induced sources that were common at high redshift.

For our proposed eMERLIN observations we select our target sample from the IR flux-limited IRAS revised Bright Galaxy catalogue (Sanders et al. 2003). This sample is extremely well observed by other instruments. In particular, it is the subject of coordinated observations by the great space observatories (HST, Spitzer, Chandra and GALAX) within the GOALS legacy project (see http://goals.ipac.caltech.edu)). For our proposed eMERLIN observations, we choose a limiting declination of +8 degrees to ensure a minimum of five hours of observations per source. Choosing this declination cut-off still allows a significant overlap with ALMA, which has array configurations designed to allow high quality imaging to at least declination $+35^{o}$ (transit elevation 32^{o}). Given the excellent high site with low atmospheric opacity, matched resolution ALMA dust continuum and spectral line imaging observations should be possible for at least half of our sample. Using the above selection criteria and parent sample we obtain a target list of 42 sources. For a number of targets we will observe multiple nuclei within eMERLIN FOV. We consider our sample size to be the minimum to allow statistical analysis and to look for trends in luminosity and/or luminosity per unit area. It also gives a sufficiently large source overlap with ALMA. Finally, it provides a large enough parent sample (see Section 4) to select a sub-group (25 objects) on the basis of first epoch images for monitoring at two further C-band epochs in order to search for powerful radio SNe to constrain the stellar IMF.

Previous MERLIN observations of our proposed sample are very fragmentary and incomplete. Some very famous sources within our sample have good published continuum maps (e.g.NGC3690/IC69, Arp220, Mrk331). Searching through the MERLIN archive we find that about one third of our targets have pipeline maps at least one wavelength with a range of sensitivities; most of these are unpublished. One of the reasons for this legacy proposal is to avoid this situation developing with eMERLIN; instead we wish to produce a complete atlas of uniform quality images of the whole sample. Uniformity of sample is very important and we do not want to omit targets because they are expected be a little too compact or a little too famous. Given the patchiness of the old MERLIN archive and the huge jump in sensitivity to eMERLIN, the best overall guide to what will be detected at eMERLIN sensitivity and resolution probably comes from VLA A-array 3.6 cm wavelength images. In particular, 25 of our target sources overlap with the 40 galaxies observed with 3.6 cm VLA array (Condon et al. 1991) at 0.25'' resolution (see Fig 1-left). This sample was chosen from the

original BGS with dec >-25^{o} and Lfir > 11.25. Although covering a similar luminosity range our samples sample is not identical with this because: (1) The two samples have different declination limits and (2) The Condon observations were selected on the basis of Lfir not Lir. Our Lir limit is 0.15 dex above the Lfir limit used by Condon. Since our sources have an average Lir of 0.12 dex above Lfir, we are roughly looking at similar intrinsic source powers but we expect source-to-source differences, (3) The Condon et al. (1991) sources were selected from the original BGS, while ours are selected from the revised BGS, which uses more accurate IRAS fluxes and a much less stringent galactic latitude limit. This latter difference is the main reason that our proposed sample, despite its more limited declination range has roughly the same size. In part we selected our sample because most modern multi-waveband observations are based on the revised BGS. Our survey will provide a complete (luminosity/declination limited) two-wavelength eMERLIN atlas of images of the revised BGS. The sample size can feasibly be observed with eMERLIN within a legacy project yet is sufficiently large for inter-comparison with other instruments.

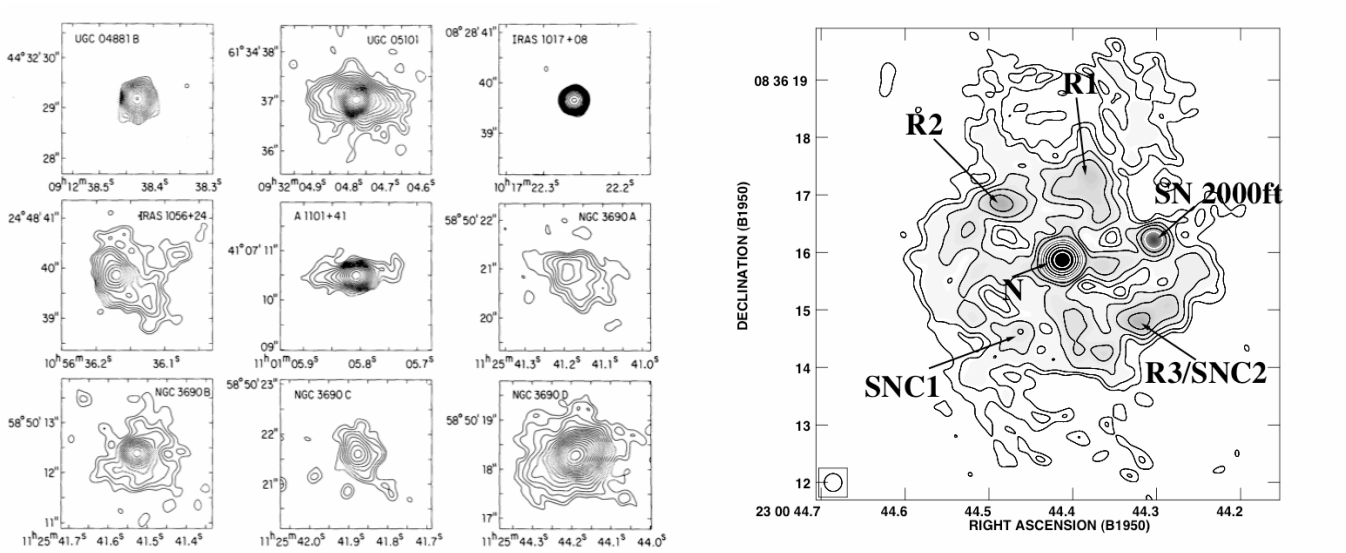

Fig 1. Left- A selection of 3.6 cm wavelength VLA-A array images with 0.25" resolution of targets from our sample (from Condon et al. 1991). These images show a typical range of source structure (note axes are in B1950 coordinates). Right- et al. A deep 3.6 cm VLA A-array image of our sample source NGC7469 with resolution 0.3" made from combining all data from 1998 through 2006 (from Perez-Torres et al. 2008). The detected powerful type II supernova SN2000ft and two other probable SNe detections (SNC1 and SNC2) are indicated. Our proposed L-band eMERLIN observations will have similar SNR towards the steep spectrum halo emission of this and other sources but with higher angular resolution. In contrast our C-band observations will resolve out most of the halo emission in this source which will more easily allow the detection of weak transient SNe.

2.2. Sample Source Properties - Although not all of our proposed sources have previously been observed in the radio at high resolution (0.25" or better), we can be confident that the eMERLIN resolution will be well matched to our goals. As noted above 25 have been observed by Condon et al. (1991) at 3.6cm wavelength, one has been observed by Kukula et al. (1995) and a final two sources were mapped by us using unpublished 8.4 GHz VLA-A (resolution 0.25") data from the NRAO archive and show structure well-matched in size to eMERLIN observations. The published 3.6 cm images at 0.25" resolution (Condon et al. 1991) show a wide range of structures (see Fig 1-left). However, many are characterized by a compact (r <= 200 pc, <300 mas) high surface brightness (Tb >= 1000 K) central radio source surrounded by a low surface brightness circum-nuclear halo (r <= 1 kpc, 1.5"). The resolution of eMERLIN is well suited to imaging both components. With 40 mas and 150 mas resolution at C- and L-band, respectively, the compact components can be resolved at both bands allowing us to probe the free-free absorption properties of these nuclei. Due to their steep spectral indices, the halo components will be optimally imaged by eMERLIN L-band, which gives higher beam SNR than the Condon 3.6 cm observations with more than twice the angular resolution. Even in cases where halo emission is not yet detected, it is possible that the eMERLIN L-band observations will detect weak radio emission from tidal tails to characterize the merger geometry of the systems or from surrounding Super Star Clusters (SSCs).

A large fraction of our targets have indications from optical spectroscopy for embedded Seyfert or LINER activity (see Section 5). Despite the fact that in some objects the radio AGN contribution can be significant, we are confident that in our sample the bulk of the radio emission is predominantly from starburst powered emission. This is shown by the analysis of the FIR-to-radio ratio at 3.6 cm within the Condon et al. (1991) sample; all except one object was found to lie on the standard correlation. Barring some strange conspiracy this implies that in nearly all cases the bulk of *both* the radio luminosity and FIR luminosity comes from star-formation. This means that we can use radio and FIR luminosities to estimate average star-formation rates and core-collapse supernova rates within our sample.

3 Diffuse radio emission

The majority of the starburst powered radio emission from our sample, in both the compact starburst cores and the halos, is expected to come from 'diffuse' synchrotron emission from energetic electrons, accelerated in supernova remnants that have diffused into the general ISM. In contrast, based on M82 and Arp 220 observations, the contribution from localized radio emission from the supernova remnants contributes only 5% (Lonsdale et al. 2006); note that at the distance of our targets and our resolution such point-like SNRs will be too weak and closely spaced to be detectable. At wavelengths without free-free absorption effects (C-band and shorter wavelength) the diffuse radio emission follows the FIR-radio correlation (see Condon et al. 1991). At least for (U)LIRGs this FIR-radio correlation is most directly explained by so-called 'calorimeter' models (e.g. Bressan et al. 2002). In these models it is assumed that electron synchrotron losses dominate over inverse-Compton losses and the starburst lifetimes are longer than this loss timescale. In this case the radio luminosity is independent of the exact value of the ISM magnetic field and depends only on the rate of input of energetic electrons from supernova explosions so giving radio luminosity proportional to star-formation rate.

3.1. Size and internal structures of starbursts - For compact (U)LIRGs radio continuum observations probably provide the best available estimates of starburst size and structure. The relativistic electrons that give rise to the diffuse radio emission have very short radiative lifetimes, because the maximum electron lifetime is 10^4 years and is set by Inverse Compton losses in the intense starburst UV field (see Condon et al. 1991; Thompson et al. 2006). If the IR-radio correlation synchrotron losses dominate over Inverse Compton losses then the electron lifetimes are even smaller than this estimate. During such very short radiative lifetimes the electrons have very little time to diffuse through the ISM and the radio observations will therefore give good estimates of the sizes of star-forming regions. Radio observations are also very difficult to obscure, even free-free absorption is not a problem at C-band, and the requisite < 0.15" resolution needed to resolve the most compact 100 pc sources at 150 Mpc is easily achieved. In contrast IR observations that are thought to be a more direct tracer of starburst activity are limited in resolution. Even more fundamentally, the bulk of the reprocessed starlight in luminous (U)LIRGs is first emitted by hot dust with spectra peaking around 25 microns, which is then almost completely absorbed and re-emitted at around 100 microns by a much larger volume of surrounding colder dust. Such reprocessing must occur since measured radio sizes are smaller than minimum FIR sizes as estimated assuming optically thick black body FIR emission (see Condon et al. 1991). High-resolution ALMA dust observations will again mainly trace the cool dust cocoon of scattered and reprocessed IR radiation.

Because of all the above observational advantages, the radio band observations of the revised BGS have a fundamental importance for finding starburst sizes and for determining structures. These starburst structures include compact (disk?) features, rings, and knots of emission from Super Star clusters (features R1 to R3 in Fig 1-right). ***Within the radio band for compact (ULIRGs eMERLIN has the right resolution/sensitivity combination to be the best instrument to obtain overall radio structures***. *Although rough size estimates are available for about half of the luminous sources in the revised BGS sample (Condon et al 1991), our proposed eMERLIN observations will have higher 6 times higher resolution and 6 times the sensitivity than those observations. Additionally our observations will give for the first-time sizes/structures for the remaining sources.* Our derived radio size information combined with observed luminosities in different wavebands will allow the determination of energy densities in these bands. In addition, before the long baselines of ALMA are available we can use the integrated lines strengths of high-density tracer molecules from single-dish mm telescopes or compact ALMA observations to estimate gas surface densities. It is very likely that the detected dense gas and the radio starburst activity are co-spatial. Furthermore, under the same assumptions total enclosed masses can be estimated from the molecular line velocity widths.

3.2. Inter-comparison with EVLA images - The enhancement of the VLA sensitivity especially in the frequency range 12 – 43 GHz will allow complementary images to be made with matched resolution to eMERLIN. These images will allow the radio spectra of (U)LIRGs to be traced at the pixel-to-pixel level. In addition, some of our target sources with extensive halo emission will greatly benefit in fidelity from combining eMERLIN and ELVA data at C-band. The broadband pixel-to-pixel spectra resulting from matched resolution eMERLIN/multi-array EVLA images at wavelengths from 20 cm to 7 mm will be able to trace a variety of physical processes. Broadband spectra can trace synchrotron absorption from compact components (a strong AGN indicator). Free-free absorption traces the thermal ionized medium. Spectral breaks at high frequency can be detected from aged electron populations. At low frequency ionization losses (Thompson 2006) can flatten spectra. Finally the ratio of thermal radio emission (measured at the VLA from 15 - 43 GHz) to synchrotron emission (measured by MERLIN) can be used as clock to date the starburst. The former emission component comes from HII regions and is proportional to the current star-formation rate while the latter comes from synchrotron emission via electrons accelerated in supernova remnants and so measures star-formation 1-10 Myr ago. The ratio of the two components can therefore be used to measuring the age of the starburst emission (Bressan 2002; Prouton et al. 2004) at each pixel .

3.3. Free-free absorption and the synchrotron/thermal fraction - Condon et al. (1991) found that while luminous (U)LIRGs at 3.6 cm obey the FIR-radio correlation the same was not true at 18 cm because of a deficit of radio emission that was ascribed to free-free absorption. Using a simple model derived from galaxy disks in which 10% of the emissivity at 1 GHz was estimated as coming from free-free emission, it was possible to roughly show that free-free absorption at 18 cm would be expected in compact (U)LIRGs. The detailed predicted spectra for such a model are shown in Figure 2, where a family of curves traces the plasma emission for increasing frequencies at which free-free opacity is unity, corresponding to different intensities of star-formation per unit area. The model predicts a correlation between radio brightness and the 18 cm to 6 cm spectral index and with the spectral curvature as measured at the two ends of C- and L-band. Our eMERLIN observations will be able to search for these correlations and so determine whether the estimated 10% fraction of thermal emission from thermal processes at 1 GHz, derived originally for galactic disks, really applies in (U)LIRGs -- or if this fraction varies from source-to-source or within sources. In some cases we expect the thermal fraction to be starburst age dependant and hence to provide an alternative route (compared to EVLA free-free short wavelength *emission* observations, see Section 3.2) to measuring starburst age as a function of position within the source. Having determined the ionised fraction by detailed fitting to the spectra, we will be able to determine per pixel the star-formation and total free-free absorption opacity. This latter quantity determines the ionized gas emission measure, which is an important constraint for interpreting Rotation Measure observations (see Section 5). Finally, we note that eLOFAR with 1500 km baselines at its highest frequency (230 MHz) will have a resolution of order 300 mas and so can be compared to tapered L-band eMERLIN maps to find spectral indices of free-free absorption regions. Such observations can constrain the clumpiness of the free-free absorbing gas.

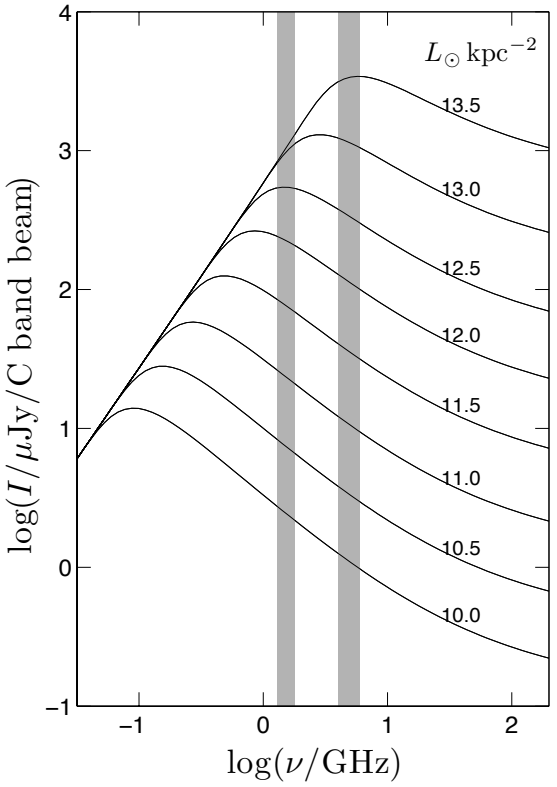

Figure 2. Model Starburst spectra for different ai SFR,eMERLIN bands plotted in grey

3.4 Testing the Kennicutt-Schmidt law and predicted maximum specific star-formation rate - Because at C-band and shorter wavelength (U)LIRGs follow the FIR-radio correlation, the observed radio brightness in mJy/solid angle can readily be converted into an area stellar luminosity (in Lsol/kpc^2). By further assuming a stellar IMF, this can be converted into a star-formation rate per unit area (in Msol/yr/kpc^2). Using these conversions eMERLIN images can be used to test whether the Kennicutt-Schmidt star-formation law still applies in dense (U)LIRG. This relation, originally derived for galactic disks, relates star-formation per unit area to gas surface density. Before resolved ALMA molecular line images are available we can estimate dense gas surface densities from single dish/compact ALMA integrated spectra of dense gas tracer molecules by assuming that this gas is spread over a source size given by the radio observations. This gas density can then be compared with the inferred star-formation per unit area derived from radio maps to check the Kennicutt law. This law is predicted to break down at some point related to the maximum area star-formation rate per unit area that can be supported in (U)LIRGs. A number of authors including Thompson et al. (2005) have argued that Eddington luminosity effects set a limiting star-formation specific area luminosity of 10^{13} to 10^{14} Lsol/kpc^2. This can be checked directly by finding the peak (non-AGN) radio brightness in our maps and converting this to Lsol/kpc^2. Thompson et al. (2005) attempted to check whether this limit applies by using data from Condon et al. (1991). With our much higher resolution and sensitivity eMERLIN images on a similar sample we will be able to check the detailed predictions of this model more critically.

4 Radio Supernovae and Stellar IMF's

4.1 Background - Observations of core-collapse supernovae (CCSNe) from stars with initial mass >8 Msol provide an alternative star-formation tracer compared to traditional ones of Hα and FIR continuum. In the optical and NIR, CCSNe are now being used as probes of the SFR at both low and high redshift (e.g. Cappellaro et al. 2005; Botticella et al. 2008) to constrain the star-formation history of the universe. However, a disadvantage of such optical/NIR SNe observations is that they can be obscured by dust which largely prevents optical/NIR SNe from being used as star-formation tracers in compact (U)LIRGs. Although SNe are much less luminous in the radio than in the optical/IR, which limits the distance to which they can be observed (to <200 Mpc until SKA), they can still be used to trace star-formation in nearby optically obscured (U)LIRGS. Recent detections of circum-nuclear and nuclear radio SNe in (U)LIRGS have been made in NGC 7469 (Colina et al. 2001; Alberdi et al. 2006), in IRAS 18293-3413 with SN 2004ip (Pérez-Torres et al. 2007), in Arp 220 with new supernovae (Parra et al. 2007), in IRAS 17138-1017 and SN 2008cs (Pérez-Torres et al. 2008).

Radio SNe emission is generated when the supernova ejecta interacts with the circum-stellar medium (CSM) formed from mass loss from the progenitor star before its explosion (Chevalier 2006; Weiler et al. 2002). Radio luminosity is therefore (unlike optical emission) a strong function of the progenitor mass loss history and hence the progenitor spectral type. It is thought that the most luminous type IIn radio SNe arise from stars with initial mass >>80 Msol (Gal-Yam et al. 2007), the less luminous SNe type IIL with mass in the range 15--25 Msol, and weak IIP SNe with mass <15Msol. Hence radio SNe studies have the potential advantage that they can be used to study the shape of the initial mass function (IMF) within (U)LIRGs. In particular, the ratio of the rate of high luminosity type IIn and IIL to the FIR luminosity (from reprocessed UV photons from Msol >8 Msol stars) should be a sensitive indicator of whether the IMF in (U)LIRGs is 'top-heavy'. We note that such ratios can also be a function of starburst age for instantaneous bursts lasting <<10 Myr, but that for most of our starbursts the dynamical constraints of orbital period and sound crossing time indicate ages of order 100 Myr.

For a long time it has been argued that the stellar IMF is a close to a universal function but recent observations suggest that this is not the case (Elmegreen et al. 2007). Theoretically it is expected that in the warm dense ISM conditions within a (U)LIRG, the IMF should indeed be top-heavy due to a larger Jeans mass (see Klessen et al. 2007). If this is true this has important implications for the star-forming history of the Universe (van Dokkum 2008) because at higher redshifts a larger fraction of the star-formation occurs in denser systems causing a redshift dependence of the conversion factors between star-formation indicators (including radio continuum) and the SFR. Observationally radio SNe observations in the dense 100pc diameter nuclei of the nearest ULIRG Arp 220 supports the idea of very unusual star-formation conditions in such objects (Parra et al. 2007). Assuming a standard Salpeter IMF the FIR luminosity implies a SFR rate of 150 Msol/yr and *total* CCSN rate of 3/yr, which in Arp220 equals the detection rate of the type IIn's. In normal galactic disks such type IIn's only occur amongst 2% - 5% of the core-collapse supernova (Gal-Yam et al 2007). Since the type IIn are supposed to come from very massive progenitors this points to an unusual top-heavy IMF. Note that the unusual results for Arp220 cannot simply be ascribed to its very dense ISM because the radio SNe occur while the ejecta is transiting the wind blown bubble generated by the progenitor. The bubble radius is set by ram pressure balance between wind and ISM pressure and scales only as the inverse square root of the ISM pressure. For estimated pressures in Arp220 and the young ages of the SNe, the ejecta radius is comfortably inside the wind blown bubble. Observationally the multi-frequency SNe light-curves (Diamond, Hurley et al., in preparation) in Arp220 are also consistent with this assumption. While its always possible that Arp220 is a unique object there are many other similar sources in our proposed sample with slightly lower FIR luminosities and surface brightness. Additionally in NGC7469 there is now strong evidence (3 powerful SNe within 8 years of monitoring Perez-Torres et al 2008 submitted) for an enhanced powerful SNe rate even within the less extreme ISM conditions found within circum-nuclear starburst rings.

We propose to monitor a subsample of our LIRGI sources at three epochs to determine the powerful radio SNe rate and determine whether the behaviour seen in Arp220 and NGC7469 is common in (U)LIRGs, which would point to unusual IMFs or stellar evolution properties. ***The eMERLIN at C-band is the optimum instrument for SNe detection in (U)LIRGS*** *only it has enough resolution to separate out SNe from the rest of the radio emission – many target nuclei are barely resolved with the ELVA at C or X bands and for higher frequency EVLA observations the detection sensitivity will be less and the SNe rise and fall times shorter than the interval between A-arrays - meaning we will miss sources and the detection rate per unit monitoring time reduced.*

4.3 Monte-Carlo Simulations - To estimate the observational possibilities of our proposed eMERLIN SNe monitoring program, we have conducted Monte Carlo simulations testing two extreme cases for radio SNe behaviour in (U)LIRGs, i.e. Case A for Arp220 like-behaviour and Case B for normal galactic disk behaviour. The simulations followed the method described in Pérez-Torres et al. 2008 and assumed a subsample of 25 sources (see Sect 4.3 for selection criteria and detailed observing strategy). The simulations used a random normal luminosity distribution with a dispersion of 0.3 dex around a mean peak value for the broad type (Ib/c or II) supernova population, and we also assumed radio light curve shapes taken from Weiler et al (1992) with rise times typical for that type/luminosity. Finally the simulations took into account that SNe explosion dates happen randomly with respect to our sampling epochs. For Case A with an Arp220-like situation, we use the empirical result that the rate of explosions of the most powerful type IIn radio SNe (luminosity same as SN2000ft and SN1986J) are approximately equal to the total CCSN rate as derived from the FIR luminosity assuming a standard stellar IMF. Although the situations may differ in other (U)LIRGs, we assumed that the fraction of type Ib/c and type II's remains the same, i.e. 26% to 74% as in galactic disks (van den Bergh et al. 2005). For Case B with normal galactic disk behaviour, we again assumed the same ratio of type Ib/c and II as before but also that 70% of type II supernova explosions are of type IIP, which are very radio weak. The remaining type IIL population (and type Ib/c's) were assumed to have moderate peak luminosity with mean luminosity similar to SN 1993J.

Table 1 shows the results of our Monte-Carlo simulation applied to a preliminary list of 25 candidate sources. Our results assume three eMERLIN observing runs at C-band, spanning two years (epoch 0 at time zero; epoch 1 after one year; epoch 2 one year after epoch 1). The calculations at C-band are made for an rms of 4 μJy/b (if Lovell is included in a 5-hr observing run, with 3.5-hr of effective ON-source-time) and for an rms of 11 μJy/b (if Lovell is NOT included). An SNR of 5 was assumed for detection. The table shows the extreme difference in predicted detection rate between Cases A and B; hence our observations should clearly be able to distinguish which of these cases applies. The simulations show the importance of three epochs of monitoring spaced one year apart. With this sampling the type II sources can be detected in their rise phase and type Ib/c in their decline phase. *Doing tests we found that if we have only two epochs either one or*

two years apart the total detection rate is roughly halved. The simulations (see Table 1) also show the importance of including the Lovell for our detection rate.

L_peak (1e27 erg/s/Hz)	Rms (mμJy/beam)	Exploded SNe SN Ib/c TOTAL	Exploded SNe SN II	Exploded SNe TOTAL	Detected SNe SN Ib/c	Detected SNe SN II	Detected SNe TOTAL
10 (all type Ib/c and type II with peak luminosity like SN2000ft - Case A)	5 (with Lovell)	12+/-3	35+/-5	47+/-7	9 +/- 3	29 +/- 5	38 +/- 6
	12 (w/o Lovell)				6 +/- 2	21 +/- 4	27 +/- 5
1 (all type Ib/c and IIL with peak luminosity like 1993J - Case B)	5 (with Lovell)				3 +/- 2	3 +/- 1	6 +/- 4
	12 (w/o Lovell)				1 +/- 1	2 +/- 1	3+/- 2

Table 1. Results of Monte Carlo simulations. First row (in blue) gives number of core-collapse SNe expected to explode in our monitored subsample of 25 sources over two years, assuming a standard Salpeter IMF. Rows two through four give numbers of SNe we predict to detect with eMERLIN C-band for different assumptions of SNe luminosity (cases A and B) and observing array (with and without Lovell). Note at the median monitored subsample distance of 130Mpc, peak SNe flux densities are 450micoJy and 45microJy for case A and B respectively

4.3 Proposed Observing strategy and follow-up - After our initial C-band imaging epoch is completed we will compile a smaller subsample of 25 target sources to monitor at a further two epochs. Optimum targets for monitoring should not be too distant because then weaker SNe will be below our detection threshold – hence we will not include sources more distant than 180 Mpc in the monitoring subsample. We will also concentrate on higher declination sources to optimise dynamic rang. Finally will also exclude those few sources (like IIIZw35), which are so compact that SNe cannot be distinguished from diffuse emission. Specifically we will exclude those sources in which more than half the C-band flux density comes from an area smaller than 25 beams (diameter <200mas). Note even for sources just above this compactness limit SNe with SN2001ft luminosity (Case A, with peak flux 450 μJy at median distance) and somewhat weaker can easily detected above the smooth radio emission of the compact component (with 500 μJy/beam). In addition in such sources all down to the weakest SN1993J-like SNe can be detected in the starburst halos. For the extremely compact starbursts we won't monitor with eMERLIN we will instead consider VLBI monitoring observations, since for these the starburst size will be small enough to be wholly within the small FOV of VLBI observations. Of course, any source that shows an off-centre compact (potential SNe) component in the initial C-band eMERLIN-imaging epoch will automatically be included in our monitoring subsample. The choice of the number of monitored sources (25) is mainly based on the minimum number needed to check the full range of predicted SNe rates (cases A to B in Table 1), while minimising our eMERLIN time request. A secondary reason for the smaller sample is to allow for the exclusion of the least suitable sources (with large distance, low declination or extreme compactness). For our Monte-Carlo simulations (see Sect 4.2), we selected the 25 sources, which already had high-resolution maps and were closest to our detection criteria.

For the SNe discovered in the survey we intend to propose additional eMERLIN (or eVLBI since they will have good positions) observations to follow their flux evolution. A quick follow-on observation immediately after detection can be used to confirm whether the SNe is a rapidly fading type Ib/c and so check the ratio of type Ib/c to type II (which may be very different in (U)LIRGs because of binary star formation/destruction in dense environments). Such post-detection monitoring will be able to measure the peak luminosity (L) and the rise time (t) of each SNe. Different classes of SNe, corresponding to different progenitor types populate different parts of L-t space (Chevalier 2006). The L-t distribution obtained for our (U)LIRG sample can eventually be compared with those obtained with unbiased radio monitoring of optically selected SNe in galactic disks (using EVLA and eMERLIN). Comparison of the obtained L-t distributions will eventually allow detailed quantitative conclusions on how stellar populations differ between (U)LIRGs and galactic disks.

5 Magnetic Fields

The strength and geometry of magnetic fields in (U)LIRGS is still an important unknown. Applying standard minimum energy arguments to the synchrotron emitting electrons, B-field strength estimates of order 100 microG are obtained (Thompson et al. 2006). For such relatively weak magnetic fields, the energy loss timescales to synchrotron radiation can be significantly larger than the loss timescale for Inverse Compton scattering off the stellar UV radiation field. Under such circumstances 'fine-tuning' is required to maintain the FIR-radio correlation because some constant small fraction of

the total input of SNR particle relativistic energy must somehow be arranged to go into radio synchrotron emission. This problem is avoided if magnetic fields are large enough to always provide the dominant energy loss mechanism. Additionally in such 'calorimeter' models the radio luminosity of a (non-instantaneous) starburst becomes independent of the exact value of the B-field (Bressan et al. 2002). Partly for this reasons Thompson et al. (2006) argue within (U)LIRGs for large (2-5 mG) B-fields, which are possible if they are in equipartition with the *thermal gas* energy density (not the relativistic particles). Recent support for such large fields comes from Zeeman splitting observations of OH megamasers, where Robishaw et al. (2008) found fields of 1-5 mG in 5 (U)LIRGs- we will try to detect more cases in our proposed eMERLIN OH observations (see Section 7).

Another approach to constraining field strengths is to observe polarization rotation measure (RMs). This is a complementary approach to OH Zeeman splitting because instead of being a point measurement it is sensitive to the integral of the B-field (times the electron density) along the line of sight. Observing RMs from the diffuse radio emission itself, even if its intrinsic polarization fraction is large, will probably not be possible at C-band because each emitting point along the LOS will have its own foreground RM giving large internal Faraday depolarization. Such a measurement may be possible in future K-band observations using selected targets derived from LIRGI. For the present proposal a more promising approach is to use a localized embedded polarized source as backgrounds. Possibilities include AGN jet/cores, anisotropic supernova or localized polarized emission from Super Star Clusters. The expected RM signal will depend on whether the foreground field is systematic or random but by analogy with galactic disks we assume a dominant systematic component. The RM also depends on the electron density distribution along the line of sight. Fortunately our C/L-band observations (see Section 3.3) will provide estimates of free-free opacity at each beam, constraining the ionized gas emission measure (EM). For a typical compact (U)LIRG which becomes optically thick to free-free absorption at 1GHz the EM=$3x10^6$ pc cm^{-3}. For this RM values can then be calculated in two limiting cases, first for ionised gas smoothly distributed over a 50 pc long LOS and secondly if concentrated into HII regions of electron density 1000 cm^{-3}. For 100 μG fields the two cases give RMs of $7x10^5$ rad/m^2 and $1.2x10^5$ rad/m^2, respectively with the RM being an order of magnitude larger for dynamically significant fields of 1 mG. Our standard continuum C-band data format will have spectral resolution 250 kHz, across this frequency interval for an RM=$1x10^5$ the polarization position angle changes by only 0.02 radians – and so there would be no problem with depolarization across our frequency channels. For the largest expected RM values channel depolarisation will however be a factor, but such high RMs can be searched for in our two C-band spectral line bands (albeit with lower sensitivity). The signal strength is hard to calculate but assuming we have a 20% polarized 1mJy AGN and requiring an SNR of 20 to detect the RM in a large space of possible values then beam sensitivities of better that10 μJy/beam are required. Using the full continuum bandwidth this is achievable comfortably only with the inclusion of the Lovell.

6 The AGN –starburst connection

A very large fraction of our targets have indications from optical spectroscopy for embedded Seyfert or LINER activity. Composite galaxies, including the Seyferts Mrk 331 and NGC7469, have central sources where the radio emission is partly starburst and partly AGN powered surrounded by starburst rings. Other clear examples of composite AGN/starburst sources in our sample include NGC 6240 (Gallimore & Beswick 2004). Despite these individual cases we expect that in most cases the AGN activity will not provide the bulk of the radio luminosity - because nearly all objects are expected to lie on the high frequency radio-FIR correlation (see Condon et al. 1991). Nevertheless the high incidence of AGN is to important for understanding possible (evolutionary?) connections between starburst and AGN activity in our (U)LIRGs. For instance, is the presence of an AGN correlated with starburst age (traced by radio continuum/spectral line clocks) or with some other property? The first task is to identify all AGNs within our sample. This can be done by using classical optical emission line diagnostics (for which there are a wealth of observations for our sample), by using complementary Chandra X-ray data, or by using the eMERLIN radio data for diagnostics (see Baan & Klöckner 2004). The advantage of radio AGN detection is that the optical AGNs can be obscured, especially if surrounded by a compact starburst. In contrast an accreting black hole always gives rise to a compact high-brightness temperature source, which is extremely difficult to obscure. Such cores or their associated jets and lobe emission can be identified in our eMERLIN data by their morphology and spectral properties. Sources with extremely high brightness temperatures (>10^5 K) are either Supernovae or AGN and the latter can be distinguished by their radio spectra and light curves. Likewise compact sources showing low frequency turnovers that can be ascribed to synchrotron self-absorption are also almost certainly AGN cores. In a study done for Lir <11.4 starbursts Parra et al. (2008, in preparation) have found a strong correlation between AGN identified by compact VLBI cores and compact starburst radio emission as measured by VLA observations. It will be interesting to see if this correlation persists for higher luminosity sources.

7 Spectral line emission/absorption

In our initial epoch C-band and L-band observations, we will configure the eMERLIN correlator to allow high-resolution observations at the expected frequencies of OH, HI and H_2CO molecular transitions in order to search for absorption and maser emission. Spatially resolved eMERLIN observations of these spectral lines will allow dynamical masses to be estimated and can be used to constrain spatial variations in chemistry and physical conditions. Although most of the

targets in our sample have been searched using single dish observations for absorption and emission and some have already been mapped with MERLIN, there are several reason why new eMERLIN spectral line observations are justified: (1) Although the main eMERLIN improvement is in continuum sensitivity the new powerful correlator will allow dual polarization *simultaneous* spectral line observations of all transitions in each band. Observing in L-band five transitions (the four OH lines plus HI) dual polarization therefore gives an increase in sensitivity of up to 3 compared to old MERLIN single-transition single-polarization observations, (2) Spectra will have higher velocity resolution giving more astrophysical detail and protection from narrow band RFI.(3) Using an interferometer weak broad emission and absorption lines are more easily detected than with single-dish because spectral baselines problems are avoided. Hence a blind search of the whole sample to look for new detections is justified. In addition, strong maser emission in single-dish spectra can be superposed in velocity on top of weak absorption, while in spatially resolved MERLIN maps (e.g. Pihlström et al. 2001) these components can be separated, (4) Not all known OH masers within our sample have been mapped with MERLIN in all transitions. It is important to make complete uniform observations of the whole sample. Using such observations in every source, we can attempt to recover all the maser flux found in extended components (Arp 220 - Rovilos et al. 2003; IIIZw35 - Pihlström et al. 2001; Mrk 231 - Klöckner et al. 2003) and compare this to compact maser emission seen with VLBI to test models (e.g. Parra et al. 2005) of the inter-relationship of these observationally diffuse and compact components. (5) With careful polarization calibration we can search for more cases of Zeeman splitting (Robishaw et al. 2008) to measure in-situ B-field strengths (a vital question see Sect 5).

From the physical point of view OH and H_2CO MM (megamaser) activity is an important characteristic of the early evolutionary stages of the nuclear starburst when there is the combination of an intense FIR radiation field and dense molecular gas in the nuclear region. Megamaser emission results from amplification of the radio continuum by excited molecular gas in the foreground. The spectral shape and the 60 μm flux density in the mid-infrared determine the pumping of the OH molecules (Baan 1989; Henkel & Wilson 1990). For the weak H_2CO MM emission the pumping scheme is not (yet) fully understood but it is likely related to the FIR radiation field (Baan et al. 1993; Araya et al. 2004). Studying spatially resolved eMERLIN maps in these transitions (especially in conjunction with future ALMA molecular line maps) will sensitively trace how the IR field and physical conditions vary across the source. High-density molecular tracers like HCN, HNC, and HCO^+ show a strong (linear) relation with the FIR luminosity (Gao & Solomon 2004; Aalto et al. 2007; Baan et al. 2008). Their relative strength relative to the more widespread CO(1-0) emission reduces steadily during the evolution of the starburst, which results from destruction and consumption of the dense ISM in the star formation process. Also the line ratios of high-density tracers such as the HCO^+(1-0)/HCN(1-0) ratio increases systematically during the course of the outburst (Baan et al. 2008). Although such changes have been attributed to the presence of an AGN in the nucleus, they are better explained by chemical and physical evolution of the ISM. One aspect that affects the line ratios containing HCO^+ is the increasing large-scale mechanical heating of the ISM resulting from SNe and SNRs (Loenen et al. 2008). Further modelling needs to be done in order to connect the integrated FIR luminosity with the sequential phenomenology of the evolving nuclear activity and the nuclear ISM during the starburst, such as the occurrence of SNe and SNRs, the atomic and molecular properties of the ISM, and the occurrence of OH MM activity. Nuclear absorption and emission lines also provide important dynamical information of the nuclear region and many sources exhibit profiles that reveal powerful outflows with velocities up to 1000km/s. Outflows with such extreme velocities in both OH and HI can only result from supernovae and their remnants. The terminal outflow velocity varies as $L_{fir}^{0.3}$, which forms a direct link with transfer of mechanical energy of the SNe to the ISM (Baan 2007).

The comprehensive study of molecular and atomic signatures via eMERLIN will contribute to the construction of a phenomenology timeline for starbursts. The occurrence of OH emission and H_2CO emission within the sample will depend on the relative age of the starburst and will reveal the physical conditions with the nuclear ISM. While previous work has focused on interpreting integrated line ratios for galaxy populations, an important legacy will be left by our MERLIN spectral line observations, which can later combined with ALMA imaging with matched resolution to obtain maximum science return from both instruments.

References

Aalto et al. 2007, A&A, 464, 193
Alberdi et al. 2006, ApJ, 638, 938
Appleton et al. 2004, ApJS, 154, 147
Araya et al. 2004, ApJS, 154, 541
Baan & Klöckner 2004, A&A, 449, 559
Baan 2007, NewAR, 51, 149
Baan et al. 2008, A&A, 477, 747
Baan et al. 1993, ApJ, 415, 140;
Baan 1989, ApJ, 338,804;
Beswick et al. 2008, MNRAS, 385, 1143
Botticella et al. 2008, A&A, 479, 49
Bressan et al 2002, A&A, 392, 377
Cappellaro et al. 2005, ApJL, 553, L19;
Chevalier 2006, astro-ph/0607422
Colina et al. 2001, ApJ, 553, L19
Condon et al. 1991, ApJ, 378, 65
Elmegreen et al. 2008, arXiv0803.3154
Gallimore & Beswick 2004, AJ, 127, 239
Gal-Yam et al 2007, ApJ, 656, 372
Gao & Solomon 2004, ApJS, 152, 63;;
Henkel & Wilson 1990, A&A, 229, 431
Klessen et al. 2007, MNRAS, 374, 29
Klöckner et al. 2003, Nature, 421, 205
Kukula et al. 1995, MNRAS, 276, 1262
Lonsdale et al. 2006, ApJ, 647, 185
Loenen et al. 2008, arXiv:0807.1728
Norris et al. 2008, arXiv0804.3998
Parra et al. 2005, A&A, 443, 383
Parra et al. 2007, ApJ, 659, 314
Perez-Gonzales et al. 2005, ApJ, 630, 82

Pérez-Torres et al. 2007, ApJL, 671, L21
Pérez-Torres et al. 2008, CBET, 1392, 2P
Pihlström et al. 2001, A&A, 377, 413
Prouton et al 2004, A&A, 421, 115
Thompson et al. 2005, ApJ, 630, 167
Thompson et al 2006, ApJ, 645, 186
Robishaw et al. 2008, ApJ, 680, 981
Rovilos et al. 2003, MNRAS, 342, 373
Sanders et al. 2003, AJ, 126, 1607
Sanders & Ishida 2004, PASP, 320,230
van den Bergh et al. 2005, PASP, 117, 773
van Dokkum 2008, ApJ, 674, 29
Weiler et al. 2002, AnnRev, 40, 387

B) Source List

Note total source flux densities at C band are expected to be 10mJy – 40mJy and at L-band 20mJy-80mJy

Name	RA	Dec	Distance Mpc	log(Lir/Lsol)
MCG+12-02-001	00 54 04.0	+73 05 13	64.28	11.44
CGCG 436-030	01 20 01.4	+14 21 35	122.02	11.63
III Zw 035	01 44 30.0	+17 06 04	106.96	11.56
NGC 0695	01 51 14.0	+22 34 55	126.7	11.63
MCG+05-06-036	02 23 21.6	+32 11 43	131.71	11.59
UGC 02369	02 54 01.9	+14 58 17	121.94	11.6
IRAS F03359+1523	03 38 48.8	+15 32 56	137.11	11.47
VII Zw 031	05 16 38.9	+79 40 11	214.83	11.94
IRAS 05223+1908	05 25 16.3	+19 10 46	116.77	11.59
MCG+08-11-002	05 40 43.3	+49 41 41	77.22	11.41
NGC 2623	08 38 23.8	+25 45 17	77.43	11.54
IRAS F08572+3915	09 00 25.0	+39 03 56	232.19	12.1
UGC 04881	09 15 54.8	+44 19 58	161.16	11.69
UGC 05101	09 35 48.8	+61 21 22	158.61	11.95
IRAS F10173+0828	10 20 00.1	+08 13 31	198.65	11.8
IRAS F10565+2448	10 59 17.4	+24 32 38	176.26	12.02
MCG+07-23-019	11 03 54.2	+40 50 58	143.21	11.61
IC 2810	11 25 47.3	+14 40 23	142.89	11.59
NGC 3690/IC 694	11 28 32.6	+58 33 40	47.74	11.88
UGC 08058	12 56 15.0	+56 52 17	171.84	12.51
VV 250a	13 15 34.9	+62 07 26	127.99	11.74
UGC 08387	13 20 34.9	+34 08 24	99.99	11.67
NGC 5256	13 38 18.2	+48 16 28	115.83	11.49
UGC 08696	13 44 41.8	+55 53 14	154.71	12.14
VV 340a	14 57 00.3	+24 37 01	139.36	11.67
VV 705	15 18 06.7	+42 44 41	168.72	11.89
IRAS F15250+3608	15 26 59.9	+35 58 34	223.49	12.02
UGC 09913	15 34 57.1	+23 30 10	79.9	12.21
NGC 6090	16 11 40.8	+52 27 27	122.55	11.51
IRAS F17132+5313	17 14 20.5	+53 10 34	204.26	11.89
NGC 6670A/B	18 33 35.6	+59 53 20	118.38	11.6
NGC 6786	19 11 01.4	+73 25 10	102.69	11.43
IRAS 19542+1110	19 56 35.4	+11 19 03	256.71	12.04
IRAS 20351+2521	20 37 18.6	+25 31 42	134.85	11.54
CGCG 448-020	20 57 23.3	+17 07 34	144.1	11.87
IRAS 21101+5810	21 11 29.3	+58 23 04	155.72	11.75
NGC 7469	23 03 15.5	+08 52 25	65.23	11.59
IC 5298	23 16 01.7	+25 33 33	108.19	11.54
NGC 7674	23 27 56.9	+08 46 46	113.64	11.5
IRAS F23365+3604	23 39 01.7	+36 21 14	251.84	12.13
IRAS 23436+5257	23 46 05.8	+53 14 00	134.78	11.51
MRK 0331	23 51 26.1	+20 35 08	70.46	11.41

C) Links to other related data sets & other legacy programs

The parent source sample from which our target list is drawn is the revised Bright Galaxy Sample (Sanders et al 2003), which is the best-studied sample of nearby powerful starbursts with extensive observations and many publications on parts of the sample or on individual objects.

In particular, the rBGS is the subject of the GOALS (Great Observatory All Sky LIRGS) NASA Great Observatories legacy program (see http://goals.ipac.caltech.edu/), which includes observations with Spitzer, Chandra, HST and GALEX.

Within GOALS Spitzer observations include 4-channel continuum imaging with IRAC (at 3.6, 4.5, 5.8 and 8 microns) and three channels of MIPS (24, 70 and 160 microns). Furthermore spectroscopy has been done in all four modes of IRS on the starburst nuclei and some companions. All of our LIRGI target sources are covered. Goals of the continuum observations are to map dust distributions of different temperatures and to relate these to galaxy interactions looking for correlations between dust colours and age. Amongst the goals of the spectroscopy programme is the identification of hidden AGNs by detection of high-ionization fine structure lines, via PAH diagnostics, and via detecting very hot (>500K) dust emission. From rotational ladders of H_2 gas the temperatures are available. Finally fine-structure line ratios are being used to age-date the starbursts and to look for high-velocity outflows. All of the above goals relate to our goals for eMERLIN imaging as described in the main science case. The HST ACS/WFC imaging observations with GOALS cover exactly the same luminosity cutoff as LIRGI Lfir >11.4 (Evans et al. program No 10592) and have goals of looking for AGN, super star clusters and host galaxy properties (Hubble type, presence of bars, etc). Chandra observations are complete for the LIRGI subsample with Lir > 11.67 and can be used to search for hidden AGN. GALEX UV observations cover Lir > 11.6 and a major goal is to calibrate what is visible from star-formation in the UV compared with other wavebands and to use as templates for interpreting redshifted UV observations of high z star forming galaxies.

In the mm and sub-mm our rBGS galaxies are the subjects of large molecular spectroscopy program led by the Leiden and Bonn groups on the Pico Veleta 30m telescope. These observations measure spectra in CO transitions (1-0, 2-1, 3-1 etc) and many high-density tracer molecules HCN, HCO^+, etc. It is expected that ALMA will have a large program to observe rBGS that will extend to Northern declinations (to allow comparison with ELVA and eMERLIN observations). Our sources will also be prime targets for multi-configuration EVLA observations from 20 cm to 7 mm wavelength that can be compared and combined with our eMERLIN data.

It is expected that with the upgrade to ELVA and eMERLIN sensitivity, there will be systematic programs of following up on optically selected supernova (and blind radio searches toward galactic disks) that will allow the construction of radio luminosity functions for SNe and fully understand the population of the luminosity. The rise-time plane occupied by different optical types (with different progenitors) can then be combined with similar data obtained for radio SNe in ULIRGs in our Legacy survey, which can only be observed by eMERLIN because of their compactness.

Within proposed eMERLIN legacy programs there are synergies with the EMERGE deep field survey (PI Muxlow) and the LeMMINGS nearby galaxy survey (PI Beswick). The LIRGI and LeMMINGs projects share a significant overlap in personnel, which is a point of strength for all programs from the point of view of science and for developing data reduction. A check shows that there are no target sources in common. This is not surprising since LeMMINGs is based on the optically selected Palomar sample of nearby galaxies and LIRGI on IRAS FIR detections of highly optically obscured system. Taken together the two projects beautifully sample the full range in the galaxy IR luminosity function (see Sanders et al 2003), with LeMMINGs sampling the 'normal' galaxy population out to log(Lir/Lsol) =11.4 and LIRGI the high luminosity tail beyond that.

D) Technical Justification

Our full sample of 42 sources will be observed during an initial epoch simultaneously at L- and C-bands in Semester 1. Based on the results of this survey we will then select an optimum sample of 25 sources for SNe monitoring at C-band only (selection to be based on distance, reasonable declination for high dynamic range and excluding the most compact sources - see science justification). These two latter C-band-only epochs will be observed in Semesters 3 and 5. At all epochs/frequency bands all sources will be observed for 5 hours (with 3.5 hrs ON source integration times) – hence the total request is 420 hrs in Semester 1 and 125 hrs in each of Semesters 3 and 5, giving a total time request of 670 hrs. With Lovell included sensitivities per source will be 9 and 4 μJy/beam respectively at L- and C-bands. At both bands we will use phase-referencing at L-band with 4 minutes on-cal and 8 minutes on-target and at C-band with 2 minutes on-cal and 8 minutes on-target. We will aim for at least 5 groups of scans per source evenly spread over hour angle to maximise

the uv-coverage. In order to detect weak SNe by image differencing, it will be an advantage to make the C-band uv-coverage for SNe monitored sources as similar as possible over the three epochs.

In the first Semester observations the L- and C-band observations will be made in full-polarisation mode (4 Stokes parameter mode). Observations will use all 16 available sub-bands of width 32 or 128 MHz correlated into 128 and 256 channels, at L- and C-band except for those dedicated for high resolution spectral line observations with 4 at L-band covering the redshifted OH mainlines (1612, 1665/1667, and 1720 MHz), one at HI (1420 MHz), and 2 at C-band covering H_2CO (4829MHz) and excited OH (6035 GHz). The Semester 3 and 5 C-band SNe monitoring observations will be pure continuum with no spectral line bands. As well as searching for SNe, the three C-band epochs will eventually be summed to produce the highest sensitivity images of those objects, that will most benefit from increased dynamic range (these sources being the higher declination non-ultra-compact sources from our sample).

For all observations we request the inclusion of Lovell telescope. Although our program can still give important results without the Lovell, its inclusion will greatly increase the science return; if a set of observations is worth doing, it is clearly worth doing the best we can. The areas in which absence of Lovell would have most impact are: (1) Reducing by 50% the detection rate of radio SNe to constrain ISM's (see Table 1 in section A); (2) Making detection of Rotation Measures impossible or marginal; (3) Seriously reducing the chance of detecting new spectral line emission/absorption features and not making improvements in sensitivity on known maser/absorption sources; and (4) Reducing the quality of images of the low brightness continuum starburst halos, which can trace tidal tails of star-formation and in which we can possibly detect new compact steep spectrum sources such as the emissions from super star clusters.

The chosen channel width described above will be sufficient such that the interferometer Field of View will extend all the way out to the edge of the Lovell primary beam (12 and 3 arcmin HPBW at L- and C-band respectively). However all of our targets are very compact; even the ones with the most extended starburst halos will extend only over a few arcseconds. This small image size will make initial imaging relatively easy, since for first goal of obtaining deep total intensity continuum images requires that we drastically averaged down our data in frequency and time, immediately after coming out of the correlator. In a few interacting galaxies (e.g IC694) there are two or more regions of radio emission but these fit within the Lovell primary beam and their positions are well known; in these cases the data can be phase rotated before being averaged in time.

For our main purpose of small field imaging, the imaged data volumes and processing requirements will not be much higher than those for the classic MERLIN. Processing will only be more challenging compared to old MERLIN in that Multi-frequency Synthesis will be used. However, note that we can always fall back and make separate images at each continuum band and sum these rather than gridding in the uv domain; this produces image fidelity intermediate between narrow band imaging and full uv gridded MFS joint deconvolution (see Conway PhD thesis 1989; Conway et al. 1991). The relatively 'vanilla' continuum initial imaging requirements of our project makes it an excellent candidate for scheduling in semester 1 of full eMERLIN operations, which is needed anyway so we can fit our SNe monitoring within the 5 semesters of legacy time.

E) Requirements for data processing and archiving

As described in part D for our first goal of deep continuum imaging should be relatively straightforward because the data can be averaged in time and frequency sown to small volume because our field of view will be quite small. One issue though is that although though are targets have total flux densities of only 10-100mJy given the high sensitivity of eMERLIN reasonably high dynamic ranges will be needed. To achieve the thermal noise if might be needed to remove distant confusing background sources within the primary beam.

If this is needed the confusing sources can be identified by delay rate mapping, data fringe rotated and mapped and these confusing data removed from the uv data before applying final fringe rotation and averaging at the position of our Target. In a few interacting galaxies (e.g. IC694) there are two or more regions of radio emission but these fit within the Lovell primary beam and their positions are well known- in these cases data can be phase rotated to multiple positions before being averaged to give a different data set for each source within the beam (of course the uv data for the whole FOV will be kept in the archive for anyone who later wants to process it to see if for instance a new object detected in another waveband is visible in the radio). For us for firs purpose of small field imaging imaged data volumes and processing requirements will not be much higher than for the old classic MERLIN. Processing will only be more challenging compared to old MERLIN in that Multi-frequency Synthesis will be used (however note that there is always the fall back of making separate images at each continuum band spectral line mode and summing these rather than gridding in the uv domain, this method produces image fidelity intermediate between narrow ban imaging and full uv gridded MFS joint deconvolution (see Conway PhD thesis 1989 and Conway et al 1991). The relatively 'vanilla' continuum initial imaging requirements of our project makes it an excellent candidate for scheduling in semester 1 of full eMERLIN operations, which is needed anyway so we can fit our SNe monitoring within the 5 semesters of legacy time.

For detection of weak SNe in our multi-epoch data we will use data differencing methods (in both uv plane and image domain) and cross self-calibration methods. In most cases we expect SNe to be bright enough relative to the noise and largely resolved out diffuse background that new sources should be easily visible just by differencing images. However

we will develop techniques to ensure that absolutely now new SNe are missed. Members of our team have extensive experience in techniques to measure small differences between multi-epoch images (Perez-Torres et al for radio SNe and Conway for motions in compact symmetric galaxies).

More challenging than deep continuum imaging or looking for source changes will be making searches for rotation measures and spectral line analysis. In both cases data has to be kept in narrow spectral channels. We intend to only do the RM search on objects where the continuum total intensity images show a compact object which could plausibly be polarized and therefore act as a background object for searching for Faraday rotation. The spectral line data will be imaged in a separate pipeline. While the initial narrow field total intensity continuum images must be ready well before semester 3 (so that we can make our final selection of the 25 sources to monitor for radio SNe) this is not the case for the polarisation or spectral line.

The PhD students involved in the continuum part of this project (Batejat, Hurley and Romero-Canizales) will work closely both with Conway (and a newly recruited software specialist in interferometric imaging at Onsala) and Rob Beswick at JBO. There is clearly a lot of synergy with the LeMMINGS imaging requirements and we hope to work closely with those in LeMMINGs working on data pipelines. Likewise a student to be recruited by Willem Baan at ASTRON will work on helping develop, optimize, and run the pipelines for spectral line data reduction for both LIRGI and LeMMINGS. Development of RM rotations using RM synthesis techniques will be done in conjunction with experts Garrington and Gabuzda on our team working with PhD students Hurley and Batejat and another student we hope to recruit.

F) Resource and Management plan

F.1 Team membership and resources

Our consortium consists brings a wide range of skills to our proposed project. Nearly all of our team members have a strong background in radio astronomy, a number have been active in algorithm development for radio imaging and have the expertise to ensure that state of the art images will be produced. The team has large sub-groups in Sweden and Spain as well as the UK (Manchester, Oxford, Liverpool) and much of the spectral line effort will be expended at ASTRON in the Netherlands. We have connections to molecular spectroscopy and millimetre observations via the inclusion of Susanne Aalto and connections to GOALS, Spitzer and Herschel via the involvement of Phil Appleton. Our team presently contains three PhD students who are (with affiliations and dates of expected PhD thesis in brackets), Rossa Hurley (OSO, 2010), Fabien Batejat (OSO 2012) and Cristina Romero-Canizales (IAA 2012). In addition, it is very likely that if our application is successful, a PhD student to work on the spectral line part of our project can be recruited at ASTRON. There are also other possibilities for recruiting students in Australia, South Africa, New Mexico and Chile. It is expected that if we are granted time, part of Hurley's PhD and most of the three other students thesis work would be dedicated to data analysis and astrophysical interpretation from the project.

At Onsala there will in early in 2009 be a major upgrade in computer facilities in support of its role as an ALMA Regional Centre (ARC) node. Pipelining and other data reduction software for eMERLIN will be installed on these machines. Additionally, the Onsala ARC node has recruited one senior permanent staff member (to start January 2009, with immediate supervisor Conway), whose role is to install and maintain software for the support of radio and millimetre interferometry data reduction. JBCA as UK eMERLIN/ALMA analysis centre has extensive computer resources. ASTRON is developing the compute-intensive LOFAR telescope project. Extensive computer facilities also exist at IAA Spain.

F.2 Organisational Structure

The consortium organisation consists of a pair or coordinators and a scheduling and initial data reduction group (Group 1) and then four specific groups (Groups 2 through 5) to produce final data products and initiate papers in the areas of continuum imaging, supernovae search, spectral-line and polarisation respectively. The two coordinators will communicate with the eMERLIN legacy committee and will rule on organisational issues including team membership. They will also mediate any disagreements between members (in the unlikely event they will arise since all team members know each other very well and are very friendly). A scheduling and initial data reduction group (Group 1 below) will interact with eMERLIN staff on the experiment scheduling and pipeline development, and will oversee the initial data reduction common to all the data products. Final data products and initial writing up of results in papers will be initiated by Groups 2 through 5 for the areas of total intensity, supernovae search, spectral line, and polarisation, respectively. Group 2 has a vital role to play in the delivery of images so that the group of monitored sources can be chosen in time for second epoch monitoring observations in Semester 3. This group therefore has a firm delivery timescale for final total intensity maps for all 42 objects at both L- and C-bands within 6 months after the end of Semester 1 observations. Groups 2 to 5 will initiate the preparation of publications. In preparing publications these groups may bring in any people from outside the collaboration, who have useful expertise or ancillary data. Note that the group memberships given below are not fixed and can be changed as the project progresses. Consortium members are free to move between groups. In addition new members can be added to the consortium upon the agreement of the coordinators. In the group memberships listed below the name order is in rough order of seniority/involvement with the first name listed being the group leader.

Gr1 Scheduling and Initial data reduction group - John Conway (OSO), Miguel Perez-Torres (IAA), Willem Baan (ASTRON), Rob Beswick (JBCA), Simon Garrington (JBCA), Rossa Hurley (OSO), Fabien Batejat (OSO), Cristina Romero-Canizales (IAA), New ASTROn student

Gr2 Total intensity continuum imaging group - John Conway (OSO), Miguel Perez-Torres (IAA), Rob Beswick (JBCA), Antxon Alberdi (IAA), Simon Garrington (JBCA), Rossa Hurley (OSO), Fabien Batejat (OSO), Cristina Romero-Canizales (IAA), Phil Diamond (JBCA), Ray Norris (CSIRO), Ylva Pihlström (UNM), Phil Appleton (Herschel Science Center, Caltech), Willem Baan (ASTRON)

Gr3 Supernova search group - Miguel Perez-Torres (IAA), John Conway (OSO), Cristina Romero-Canizales (IAA), Fabien Batejat (OSO), Rob Beswick (JBCA), Antxon Alberdi (IAA), Miguel Perez-Torres (IAA), Luis Colina (DAMIR, Madrid) , Jose-María Torrelles (CSIC-IEEC, Barcelona), Phil Diamond (JBCA), Willem Baan (ASTRON)

Gr4 Spectral line group - Willem Baan (ASTRON), John Conway (OSO), Phil Diamond (JBCA), Rob Beswick (JBCA), Hans-Rainer Klockner (Oxford), ASTRON student, Susanne Aalto (OSO), Carole Mundell (Liverpool, JM), Phil Appleton (Herschel Science Center, Caltech), Rodrigo Parra (Catolica U), Ylva Pihlström (UNM),

Gr5 Polarisation group - John Conway (OSO), Simon Garrington (JBCA), Denise Gabuzda (UC Cork), Fabien Batejat (OSO)

G) Justification of legacy status

High-luminosity nearby starbursts in the local universe are clearly of great interest to the community as witnessed by the number of publications in this area, conferences, etc. It has been a great pity that even though Classic MERLIN had much unique information to contribute (on starbursts sizes, structures etc), the impact has been diluted because only small samples or singles sources were mapped. This is in contrast to other wavebands were large coherent programmes are completed or are underway (see part C). We want to avoid this situation with eMERLIN. Given that good quality imaging with MERLIN takes relatively long per source, the only ways to image a large enough sample (42 sources) is to use the Legacy project vehicle. In the process, our data set will provide a number of specific legacies to the community. First, a complete set will be produced of data ready and waiting to be combined with EVLA data, when it comes on line. Likewise, follow-up VLBI studies (using EVN and global stations and 4 eMERLIN stations using eVLBI and 1Gbit/s data rates) at high sensitivity will complement and augment the eMERLIN data. The data and maps will also be made available to compare with high-resolution ALMA for sources in the declination range +8 to +35 deg.

……..